Journal of Education for Pure Science- University of Thi-Qar
Vol.14, No. 3 (2024)
Website: jceps.utq.edu.iq Email: jceps@eps.utq.edu.iq

DOI: https://doi.org/10.32792/jeps.v14i3.442

A Modified of Fourth-Order Partial Differential Equations Model Based on Isophote Direction to Noise Image Removal

Zahra R. Jawad[1], Ahmed K. Al. Jaberi[2]

1,2 Department of Mathematics, College of Education for Pure Science, University of Basrah, Basrah, Iraq

Email address of the Corresponding Author: ahmed.shanan@uobasrah.edu.iq

Received 2/6/2024, Accepted 28/7/2024, Published 01 / 09/2024

Abstract

Image processing is a challenging task in the field of computer vision. Fourth-order equations are a powerful tool for removing noise, as they can avoid the block effect typically seen in second-order equations. In addition, these equations show high efficiency in high-frequency regions. This paper suggests combining the direction of isophote and fourth-order partial differential equations to reduce the problem of edges loss and preserve important details of the image. The direction of the isophote can regulate the direction of diffusion. Thus, we have a proposed model that can remove the noise in the area while preserving the important edges and details of the image. We have proven the efficiency and superiority of the proposed model by applying it to a set of images and solving it numerically using the finite difference method (FDM).

Keywords

Image denoising; fourth-order partial differential equations; nonlinear filtering; isophote direction; finite difference method

1. Introduction

Image denoising is one of the initial stages of image processing. Many models based on the diffusion method have been used to smooth the image. It is known that the diffusion force is more effective in areas of high frequency. So, one of the problems, we face in the model based on the diffusion method is its possible loss of edges. Amongst many image-denoising methods, the use of partial differential equations (PDES) plays a significant role in the process due to their high efficiency without any prior knowledge and their high ability to preserve image edges. Models based on partial differential equations and techniques for solving them have garnered attention due to their numerous applications in diverse domains, including engineering [1, 2] and medicine [3]. In the image processing process, these methods rely on either the axiomatic approach of nonlinear diffusions [4] or the variational approach of energy functional minimization [5, 6]. Anisotropic diffusion equations, introduced by Perona and Malik [7], remain among the most widely used and effective techniques for image denoising. The authors of [7] suggested taking into account the Perona Malik (PM) second-order PDE, a second-order non-linear diffusion model. Although it is efficient, it causes a block effect that gives the image a distorted appearance. This problem was solved by You and Kaveh [8], who introduced a new fourth-order model to reduce image noise, where he replaced the gradient operator in the PM second-order PDE model with the Laplace operator. We have noticed an increase in studies recently that rely on fourth-order models due to their advantages and efficiency in reducing oscillation in high-frequency regions. We have observed many studies that rely on these models in the process of reducing medical image noise [9, 10]. Also, Yadava and Srivastava proposed a fourth-order model to remove Poisson noise from microscopic lung biopsy images, and to improve the model, it was multiplied by the maximum likelihood estimate [11].

For the first time, Bavirisetti introduced a fourth-degree partial differential equation for use in the image-merging process [12]. Calatroni investigated the application of directional splitting techniques to fourth-order nonlinear diffusion problems [13]. Laghrib proposed a new model based on fourth-order differential equations, combining the features of Berona Malik's diffusion model [7] in flat places and the Wickert model near boundaries with a higher order of diffusion [14]. Ying developed the LLT model, whose high-order PDE-based approach was first proposed by Lysaker, Lundervold, and Tai [15] by adding a weighted function [16]. Khoeiniha proposed a model based on fourth-order differential equations with elastic parameters determined using the optimal control problem, thus being adaptable to any application [17]. Because the second-order PDEs' evolution weakens in high-frequency regions, the fourth-order PDEs are better at suppressing oscillation at high frequencies than the second-order PDEs. Therefore, as mentioned before, we may lose some details in the images processed using models based on fourth-degree equations under the diffusion process. Consequently, we proposed a model that combines fourth-degree equations and the direction of the isophote.

This paper proposes a new fourth-order differential equation denoising model to deal with different types of noise in images. The model was built by combining the YK model and isophote operator, enabling the denoising method to remove the noise and preserve the edges and corners in the images without artifacts; more details can be found in Section 4. The rest of the paper is organized as follows: Section 2 presents a fourth-order differential equation (YK) model for image noise reduction. Section 3 displays the concept of the isophote operator. Section 4 introduces the proposed model for reducing image noise. Several numerical results of the proposed model and other models for image noise reduction have been presented and compared, and the conclusions will be discussed and presented in Section 5. Finally, conclusions and future works are introduced in Section 6.

2. Fourth-order PDE model (YK model)

It was introduced in 2000 by You and Kaveh [8], unlike the approximation in smooth constant second-order PDE, fourth-order PDE will evolve and settle down to a piecewise smooth picture if the image support is infinite. It is widely recognized that piecewise smooth images appear more natural than piecewise constant images. As a result, the block effects will be decreased, leaving the image looking more natural. The optimization formula is presented as follows:

$$\min_{u}\{\int_{\Omega} ||f-u|| + \|\Delta u\|\} \; d\Omega \qquad (1)$$

Where Δ denoted Laplacian operator, f is a noise image, u is a denoising image. This formula is solved using the Euler-Lagrange equation as follows:

$$-\Delta[c|\Delta u|\Delta u] + (f-u) = 0 \qquad (2)$$

Using the Gradient descent method on above equation (2) as below:

$$\frac{\partial u}{\partial t} = -\Delta[c|\Delta u|\Delta u] + (f-u) \qquad (3)$$

Another advantage of this model is that it can successfully suppress oscillations in high-frequency regions, unlike second-order models. When using several functional behaviors in the formulation, there is flexibility available [18].

3. Direction of isophote Operator

The lines of similar intensity in a 2D image and the surfaces of equal intensity in a 3D image are known as isophotes [19], which means an isophote is a curve on an image connecting points of equal brightness. In [20], the direction of the isophote operator is defined as follows:

$$\nabla^{\perp}u(x,y) = \left(-\frac{\partial}{\partial y}, \frac{\partial}{\partial x}\right)u(x,y) \qquad (4)$$

Where $u(x,y)$ presents the color value of the point (x,y).

4. YK-I Proposed Model

The fundamental tenet of the model is that to preserve the edge, the isophote direction operator should constantly extend into the area that has to be repaired after reaching the region border. So, we combined between YK model to smooth the area and direction of the isophote operator to regulate the direction of diffusion. This model is given as follows:

$$\frac{\partial u}{\partial t} = -\Delta[c|\Delta u|\Delta u] + \lambda\, \nabla u \qquad (5)$$

Where the λ is a parameter used to control the direction and amount of information diffusion. An iterative method can be used to numerically solve equation (5). Considering a space grid size of h=Δx=Δy and a time step size of we quantize the space and time coordinates as follows:

$$t = n\Delta t, \quad n = 0,1,2 \ldots \qquad (6)$$

$$x = ih, \quad i = 0,1,2 \ldots I \qquad (7)$$

$$y = jh, \quad j = 0,1,2 \ldots J \qquad (8)$$

where the picture support size is expressed as $ih \times jh$. The Laplacian of the image intensity function is given as follows

$$\Delta u_{i,j}^{n} = \frac{u_{i+1,j}^{n} + u_{i-1,j}^{n} + u_{i,j+1}^{n} + u_{i,j-1}^{n} - 4u_{i,j}^{n}}{h^2} \qquad (9)$$

with symmetric boundary conditions

$$u_{-1,j}^{n} = u_{0,j}^{n}, \qquad u_{I+1,j}^{n} = u_{I,j}^{n} \quad j = 0,1,2, \ldots J \qquad (10)$$

$$u_{i,-1}^{n} = u_{i,0}^{n}, \qquad u_{i,J+1}^{n} = u_{i,J}^{n}, \qquad i = 0.1.2, \dots I \tag{11}$$

$$let\ A(\Delta u) = C(|\Delta u|\Delta u) \tag{12}$$

as

$$A_{i,j}^{n} = A\left(\Delta u_{i,j}^{n}\right) \tag{13}$$

the Laplacian of the $B_{i,j}^{n}$ is given as follows:

$$\Delta A_{i,j}^{n} = \frac{A_{i+1,j}^{n} + A_{i-1,j}^{n} + A_{i,j+1}^{n} + A_{i,j-1}^{n} - 4A_{i,j}^{n}}{h^2} \tag{14}$$

with symmetric boundary conditions

$$A_{-1,j}^{n} = A_{0,j}^{n}, \qquad A_{I+1,j}^{n} = A_{I,j}^{n} \qquad j = 0,1,2, \dots J \tag{15}$$

$$A_{i,-1}^{n} = A_{i,0}^{n}, \qquad A_{i,J+1}^{n} = A_{i,J}^{n}, \qquad i = 0.1.2, \dots I \tag{16}$$

$$let\ B = \left(-u_y, u_x\right) \tag{17}$$

as

$$B_{i,j}^{n} = \left(\frac{u_{i,j}^{n} - u_{i,j+1}^{n}}{h}\ , \frac{u_{i+1,j}^{n} - u_{i,j}^{n}}{h}\right) \tag{18}$$

finally, the numerical approximation of equation (5) is provided as:

$$u_{i,j}^{n+1} = u_{i,j}^{n} - \Delta t\ \Delta A_{i,j}^{n} + \Delta t\ \lambda\ B_{i,j}^{n} \tag{19}$$

5. Numerical Experiments And Results

The proposed fourth-order model was implemented and solved numerically using the FDM method [8] on 100 color images from the Berkeley database [21], where they represent the low- and high-texture color images, as seen in Figure 1. The numerical solutions of the YK-I model were compared with obtained results using the YK model using statistical

quality measures (SQMs), such as mean square error (MSE), peak signal-to-noise ratio (PSNR) [22], structural similarity index (SSIM) [23, 24], and entropy of original (E_o) and denoised (E_d) image Which represent quantitative measurements of disturbance in the image. These (SQMs) are used to evaluate the efficiency and effectiveness of the model in terms of its ability to preserve image texture, the taken time to obtain results was also studied. The noise removal procedure was implemented in MATLAB code, where (elapsed for MATLAB, version R2023a, running on a 2.11 GHz, Intel core i5-10210U CPU laptop with 1.60GHz of L2 memory and 8G of RAM). Three experiments were conducted in this section. The experiment of analyzing the behavior of models with different types of noise is introduced in section 5.1; the experiment of analyzing the behavior of models with different noise levels is displayed in section 5.2, and the experiment of analyzing the behavior of models with different iterations of the digital process is presented in section 5.3.

Figure 1. Example of eight out of 100 training natural images.

5.1. Different types of noise

This section discusses how the proposed model behaves with different types of noise such as Gaussian, Poisson [25], salt & pepper [26, 27], and speckle [28, 29], as shown in Figure 2. This was performed based on the standard noise ratio and the value of λ is 0.0001, and the iteration of the numerical process was 100. The results of the YK-I model were compared with the obtained results using the YK model. Tables 1–4 provide the analysis

of (Yk) and (YK-I) models by showing the values of MSE, PSNR, SSIM, and entropy for different types of noise as well as the computation time.

SQMs	MSE	PSNR	SSIM	E_o	E_d	TIME(S)
YK	82.37074	29.02173	0.368449	7.144132	7.449229	0.87757
YK-I	43.06723	32.00343	0.65021	7.144132	7.141616	1.397505

Table 1. Models analysis when the Gaussian noise.

SQMs	MSE	PSNR	SSIM	E_o	E_d	TIME(S)
YK	35.04768	32.87746	0.735034	7.144132	7.269202	0.972698
YK-I	34.04465	33.25688	0.724246	7.144132	7.050174	1.558207

Table 2. Models analysis when the Poisson noise.

SQMs	MSE	PSNR	SSIM	E_o	E_d	TIME(S)
YK	6.381876	40.13152	0.409725	7.144132	7.143245	0.846464
YK-I	28.61177	34.18429	0.745159	7.144132	7.014932	1.364674

Table 3. Models analysis when the salt & pepper noise.

SQMs	MSE	PSNR	SSIM	E_o	E_d	TIME(S)
YK	76.78437	29.47579	0.481419	7.144132	7.350486	0.812736
YK-I	53.24902	31.10851	0.633186	7.144132	7.094158	1.130258

Table 4. Models' analysis when the speckle noise.

(a) Gaussian noise (b) Poisson noise (c) salt & pepper noise (d) speckle noise

Figure 2. Different types of standard ratio noise.

The advantages of the suggested approach over the YK model are readily apparent, as is its capacity to manage many kinds of noise, including Gaussian, Poisson, and Speckle

noise. The two images are more similar and of greater quality, as evidenced by the noticeable decrease in the mean squared error ratio and increase in the PSNR ratio. As for entropy, compared to the YK model, the YK-I model entropy is closer to that of the original image. Additionally, we note that the two images' structural similarity is indicated by a greater SSIM ratio. A special case should be paid to salt and pepper noise, where we observe an increase in the squared error ratio. Still, there is a clear increase in the SSIM ratio, which indicates a significant structural improvement in the YK-I model, as shown in Figure 3.

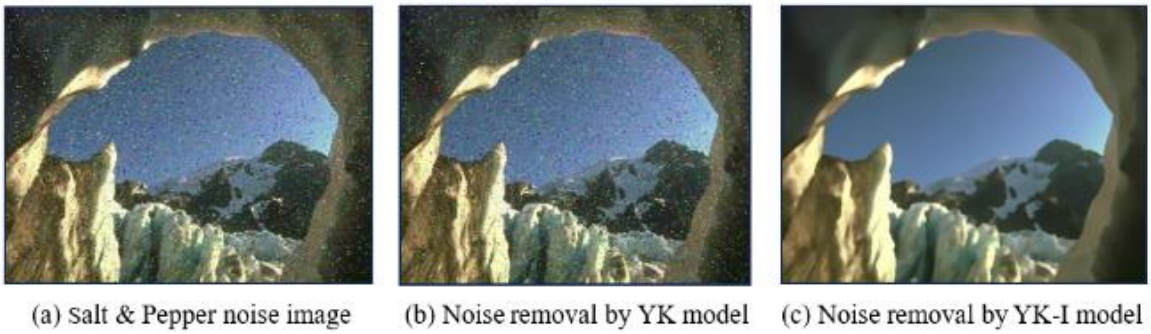

(a) Salt & Pepper noise image (b) Noise removal by YK model (c) Noise removal by YK-I model

Figure 3. Salt & Pepper noise removal image.

5.2. Different ratios of added noise

This section discusses how the proposed model behaves across four noise levels: 0.1, 0.2, 0.3, and 0.4, as shown in Figure 4. This was performed based on the salt and pepper noise and the value of λ is 0.0001, and the iteration of the numerical process was 300. The results were compared with the YK model. Tables 5–8 provide the analysis results of (YK) and (YK-I) models by showing the values of MSE, PSNR, SSIM, and entropy for four noise levels as well as the computation time.

SQMs	MSE	PSNR	SSIM	E_o	E_d	TIME(S)
YK	50.94918	31.19683	0.237168	7.144132	7.298161	16.06824
YK-I	42.41315	32.21696	0.611037	7.144132	6.951409	22.19715

Table 5. Models analysis when the salt & pepper noise ratio is 0.1.

SQMs	MSE	PSNR	SSIM	E_o	E_d	TIME(S)
YK	65.29566	30.09553	0.135977	7.144132	7.442206	14.47611
YK-I	42.81551	32.1679	0.60571	7.144132	6.956847	21.42959

Table 6. Models analysis when the salt & pepper noise ratio is 0.2.

SQMs	MSE	PSNR	SSIM	E_o	E_d	TIME(S)
YK	75.96078	29.44104	0.092648	7.144132	7.528283	14.52023
YK-I	43.34191	32.10481	0.599253	7.144132	6.964528	21.56208

Table 7. Models analysis when the salt & pepper noise ratio is 0.3.

SQMs	MSE	PSNR	SSIM	E_o	E_d	TIME(S)
YK	84.08089	29.00537	0.066561	7.144132	7.56053	16.91997
YK-I	44.01248	32.02594	0.592564	7.144132	6.973421	24.32754

Table 8. Models' analysis when the salt & pepper noise ratio is 0.4.

(a) A ratio is 0.1 (b) A ratio is 0.2 (c) A ratio is 0.3 (d) A ratio is 0.4

Figure 4. Different ratios of added salt & pepper noise.

Even though we see an inverse relationship between model efficiency and noise ratio in this subsection, we can also see how good YK-I model is and how it can adapt and evolve to different noise levels by looking at the statistical values and noting the higher PSNR and SSIM and lower mean square error ratio when compared to the YK model. Additionally,

the YK-I model's entropy is closer to the original image's entropy than the YK model. It can be visually observed that YK-I model outperforms the YK model from the results shown in Figure 5, which clearly highlight the model's performance.

(a) Salt & Pepper noise image (b) Noise removal by YK model (c) Noise removal by YK-I model

Figure 5. Salt & Pepper noise removal when the ratio is 0.4.

5.3. Different iterations of numerical solutions

In this section, the behavior of the proposed model is studied over different iterations of the numerical process: 100, 300, 500, and 700, as shown in Figure 6. Based on salt and pepper noise, the value of λ is 0.0001, and a noise ratio of 0.4. The results were compared with the YK model.

(a) An iteration is 100 (b) An iteration is 300 (c) An iteration is 500 (d) An iteration is 700

Figure 6. Salt & Pepper noise removal using YK-I model with different iterations process.

Tables 9–12 provide the YK and YK-I models' analysis by showing the results of some statistical quality measures across four different iterations of the numerical process as well as the computation time.

SQMs	MSE	PSNR	SSIM	E_o	E_d	TIME(S)

YK	60.15364	30.40401	0.059471	7.144132	7.090079	4.931557
YK-I	38.24024	32.71599	0.638706	7.144132	7.003164	7.477763

Table 9. Models analysis when the iteration of the numerical process is 100.

SQMs	MSE	PSNR	SSIM	E_o	E_d	TIME(S)
YK	84.08089	29.00537	0.066561	7.144132	7.56053	16.91997
YK-I	44.01248	32.02594	0.592564	7.144132	6.973421	24.32754

Table 10. Models analysis when the iteration of the numerical process is 300.

SQMs	MSE	PSNR	SSIM	E_o	E_d	TIME(S)
YK	86.14521	28.9453	0.074934	7.144132	7.663312	23.18683
YK-I	47.41221	31.6612	0.56914	7.144132	6.953219	38.99474

Table 11. Models analysis when the iteration of the numerical process is 500.

SQMs	MSE	PSNR	SSIM	Eo	Ed	TIME(S)
YK	83.86054	29.1105	0.085153	7.144132	7.654805	32.46879
YK-I	50.0117	31.40124	0.55369	7.144132	6.936225	49.00545

Table 12. Models' analysis when the iteration of the numerical process is 700.

This subsection describes the inverse relationship between model efficiency and the number of iterations, where the YK-I model performs better at low iterations as shown in Figure 6, and it is clear from the low MSE ratio as well as the high PSNR and SSIM ratio. Also, the entropy value closest to the original image was at the lowest iterations. The YK-I model consistently outperforms the YK model between iterations. It can be visually observed that YK-I model outperforms the YK model from the results shown in Figure 7, which highlight the model's performance.

(a) image noise (b) Noise removal by YK model (c) Noise removal by YK-I model

Figure 7. Salt & Pepper noise removal when the iteration of the numerical process is 100

6. Conclusions and Future Works

To lessen the issue of missing edges and significant details in the image, this research suggested a new model that blends the direction of the isophote operator with a fourth-order partial differential equation. the SQMs were used to compare the outcomes of multiple numerical experiments with the YK model to demonstrate the effectiveness of the proposed model. We examined MSE, PSNR, SSIM, and ENTROPY. These SQMs allowed to see that the proposed model outperforms the YK model in handling various kinds of noise and adjusting to varying noise ratios without compromising its performance. Additionally, we discovered an inverse correlation between the proposed model efficiency and the number of iterations, leading to the conclusion that the model proposed reaches a steady state with a few iterations. In the future, the YK-I can be applied to another dataset to study and check its performance. The YK-I model can also be theoretically studied to prove its uniqueness, stability, and existence. On the other hand, different operators may be used with a fourth-order equation to introduce a new model for noise removal in images.

References

[1] Al-Griffi, T. A. J., & Al-Saif, A. S. J. (2022). Yang transform–homotopy perturbation method for solving a non-Newtonian viscoelastic fluid flow on the turbine disk. ZAMM-Journal of Applied Mathematics and Mechanics/Zeitschrift für Angewandte Mathematik und Mechanik, 102(8), e202100116.

[2] Abdul-Ameer, Y. A., & Ali Al-Saif, A. S. J. (2023). Fourier-homotopy perturbation method for heat and mass transfer with 2D unsteady squeezing viscous flow problem. Journal of Computational Applied Mechanics, 54(2), 219-235.

[3] Al–Sadi, R. O., & Al-Saif, A. S. J. (2023). Development and simulation of a mathematical model representing the dynamics of type 1 diabetes mellitus with treatment. Partial Differential Equations in Applied Mathematics, 8, 100575.

[4] Chan, T. F., & Esedoglu, S. (2005). Aspects of total variation regularized L 1 function approximation. SIAM Journal on Applied Mathematics, 65(5), 1817-1837.

[5] Strong, D., & Chan, T. (2003). Edge-preserving and scale-dependent properties of total variation regularization. Inverse problems, 19(6), S165.

[6] koenderink, J. J. (1984). The structure of images. Biological cybernetics, 50(5), 363-370

[7] Perona, P., & Malik, J. (1990). Scale-space and edge detection using anisotropic diffusion. IEEE Transactions on pattern analysis and machine intelligence, 12(7), 629-639

[8] You, Y. L., & Kaveh, M. (2000). Fourth-order partial differential equations for noise removal. IEEE Transactions on Image Processing, 9(10), 1723-1730

[9] Vanitha, K., Satyanarayana, D., & Prasad, M. G. (2019, July). A new hybrid medical image fusion method based on fourth-order partial differential equations decomposition and DCT in SWT domain. In 2019 10th International Conference on Computing, Communication and Networking Technologies (ICCCNT) (pp. 1-6). IEEE.

[10] Wang, Y., Ji, X., & Dai, Q. (2010). Fourth-order oriented partial-differential equations for noise removal of two-photon fluorescence images. Optics letters, 35(17), 2943-2945

[11] Yadava, P. C., & Srivastava, S. (2024). Denoising of Poisson-corrupted microscopic biopsy images using a fourth-order partial differential equation with ant colony optimization. Biomedical Signal Processing and Control, 93, 106207

[12] Bavirisetti, D. P., Xiao, G., & Liu, G. (2017, July). Multi-sensor image fusion based on fourth-order partial differential equations. In 2017 20th International Conference on Information Fusion (Fusion) (pp. 1-9). IEEE

[13] Calatroni, L., Düring, B., & Schönlieb, C. B. (2013). ADI splitting schemes for a fourth-order nonlinear partial differential equation from image processing. arXiv preprint arXiv:1305.5362

[14] Laghrib, A., Chakib, A., Hadri, A., & Hakim, A. (2020). A nonlinear fourth-order PDE for multi-frame image super-resolution enhancement. Discrete & Continuous Dynamical Systems-B, 25(1), 415

[15] Lysaker, M., Lundervold, A., & Tai, X. C. (2003). Noise removal using a fourth-order partial differential equation with applications to medical magnetic resonance images in space and time. IEEE Transactions on image processing, 12(12), 1579-1590

[16] Ying, W., Jiebao, S., & Zhichang, G. (2022). A new anisotropic fourth-order diffusion equation model based on image features for image denoising. Inverse Problems and Imaging, 16(4), 895-924

[17] Khoeiniha, N., Hosseini, S. M., & Davoudi, R. (2021). Trainable fourth-order partial differential equations for image noise removal. Iranian Journal of Numerical Analysis and Optimization, 11(2), 235-260

[18] Liu, X. Y., Lai, C. H., & Pericleous, K. A. (2015). A fourth-order partial differential equation denoising model with an adaptive relaxation method. International Journal of Computer Mathematics, 92(3), 608-622

[19] Kim, J. B., & Kim, H. J. (2003). GA-based image restoration by isophote constraint optimization. EURASIP Journal on Advances in Signal Processing, 2003, 1-6

[20] Sun, X., & Xu, C. (2009, December). Image denoising and inpainting model based on Taylor expansion. In 2009 International Conference on Computational Intelligence and Security (Vol. 1, pp. 666-670). IEEE

[21] C. F. and D. M. Pablo Arbelaez, "The Berkeley Segmentation Dataset and Benchmark," 2007. The website of the Berkeley database is https://www2.eecs.berkeley.edu/Research/Projects/CS/vision/bsds/

[22] Bovik, A. C. (2010). Handbook of image and video processing. Academic press

[23] Wang, Z., Bovik, A. C., Sheikh, H. R., & Simoncelli, E. P. (2004). Image quality assessment: from error visibility to structural similarity. IEEE transactions on image processing, 13(4), 600-612

[24] Gu, K., Wang, S., Zhai, G., Lin, W., Yang, X., & Zhang, W. (2016). Analysis of distortion distribution for pooling in image quality prediction. IEEE Transactions on Broadcasting, 62(2), 446-456

[25] Rodrigues, I., Sanches, J., & Bioucas-Dias, J. (2008, October). Denoising of medical images corrupted by Poisson noise. In 2008 15th IEEE International Conference on Image Processing, pp. 1756-1759.

[26] Liang, H., Li, N., & Zhao, S. (2021). Salt and pepper noise removal method based on a detail-aware filter. Symmetry, 13(3), 515.

[27] Chan, R. H., Ho, C. W., & Nikolova, M. (2005). Salt-and-pepper noise removal by median-type noise detectors and detail-preserving regularization. IEEE Transactions on Image Processing, 14(10), 1479-1485.

[28] Maity, A., Pattanaik, A., Sagnika, S., & Pani, S. (2015, January). A comparative study on approaches to speckle noise reduction in images. In 2015 International Conference on Computational Intelligence and Networks (pp. 148-155). IEEE.

[29] Jaybhay, J., & Shastri, R. (2015). A study of speckle noise reduction filters. signal & image processing: An international Journal (SIPIJ), 6(3), 71-80.